Band engineering and growth of tensile strained Ge/(Si)GeSn heterostructures for tunnel field effect transistors

S. Wirths, A. T. Tiedemann, Z. Ikonic, P. Harrison, B. Holländer et al.

Citation: Appl. Phys. Lett. **102**, 192103 (2013); doi: 10.1063/1.4805034
View online: http://dx.doi.org/10.1063/1.4805034
View Table of Contents: http://apl.aip.org/resource/1/APPLAB/v102/i19
Published by the American Institute of Physics.

Band engineering and growth of tensile strained Ge/(Si)GeSn heterostructures for tunnel field effect transistors

S. Wirths,[1] A. T. Tiedemann,[1] Z. Ikonic,[2] P. Harrison,[2] B. Holländer,[1] T. Stoica,[1] G. Mussler,[1] M. Myronov,[3] J. M. Hartmann,[4] D. Grützmacher,[1] D. Buca,[1] and S. Mantl[1]
[1]*Peter Grünberg Institute 9 (PGI 9) and JARA-Fundamentals of Future Information Technologies, Forschungszentrum Juelich, 52425 Juelich, Germany*
[2]*Institute of Microwaves and Photonics, School of Electronic and Electrical Engineering, University of Leeds, Leeds LS2 9JT, United Kingdom*
[3]*Department of Physics, University of Warwick, Coventry CV4 7AL, United Kingdom*
[4]*CEA, LETI, MINATEC Campus, 17 rue des Martyrs, 38054 Grenoble, France*

(Received 19 February 2013; accepted 30 April 2013; published online 14 May 2013)

In this letter, we propose a heterostructure design for tunnel field effect transistors with two low direct bandgap group IV compounds, GeSn and highly tensely strained Ge in combination with ternary SiGeSn alloy. Electronic band calculations show that strained Ge, used as channel, grown on $Ge_{1-x}Sn_x$ ($x > 9\%$) buffer, as source, becomes a direct bandgap which significantly increases the tunneling probability. The SiGeSn ternaries are well suitable as drain since they offer a large indirect bandgap. The growth of such heterostructures with the desired band alignment is presented. The crystalline quality of the (Si)Ge(Sn) layers is similar to state-of-the-art SiGe layers. © *2013 AIP Publishing LLC*. [http://dx.doi.org/10.1063/1.4805034]

The development of group IV heterostructures has evoked significant interest not only for boosting the performance of metal oxide field effect transistors (MOSFETs) but also of advanced devices, such as tunnel field effect transistors (Tunnel-FETs). These tunneling devices are capable to switch-on at smaller gate voltages, since inverse subthreshold slopes below 60 mV/dec become feasible. The physics behind this phenomenon is the carrier injection into the transistor channel via band-to-band-tunneling (BTBT), rather than thermal emission. BTBT in an *n*-Tunnel-FET implies that electrons from the p^+-source valence band tunnel across the bandgap, acting as a potential barrier, to the conduction band of the intrinsic channel (and holes tunnel in the opposite direction). This concept allows to cut-off the high energy tail of the source Fermi distribution and hence to effectively cool down the electronic system.[1,2] Steeper slopes enable reduction of the device supply voltage paving the way for energy efficient switching. In indirect semiconductors like Si, Ge, and their alloys, where the indirect bandgap, E_G (G = L, X, or Δ) is much smaller than the direct bandgap E_Γ, indirect tunneling is the main tunneling process. The required change of momentum of the tunneling particle here occurs via phonon absorption/emission while no phonon is required in direct Γ→Γ band-to-band tunneling, which significantly increases the tunneling probability. Recent simulations[3] indicate that Ge and GeSn,[4] which offer much lower bandgaps and smaller carrier effective masses, boost the Tunnel-FET performance due to an increased contribution of direct transitions.[5] While the bandgap engineered III/V heterostructures for Tunnel-FETs have been theoretically and experimentally investigated,[6] Si based direct bandgap Tunnel-FETs still lack of suitable materials for their realization.

Here, we propose a Si compatible heterostructure tailored for vertical Tunnel-FETs. The idea is to exploit the properties of two direct bandgap group IV semiconductors, GeSn and tensely strained Ge, as source and channel, respectively, in combination with an indirect SiGeSn alloy as drain. The calculated electronic band diagram for such a structure is shown in Fig. 1(a). The bandgaps and band-offsets of the strained Ge on relaxed binary $Ge_{1-x}Sn_x$ alloys layers as well as the ternary $Si_yGe_{1-x-y}Sn_x$ layers have been calculated from the supercell empirical pseudopotential method[7] (the results of which have been used to find quadratic fitting expressions[8]), together with linear interpolation of deformation potentials and band offsets of elemental Si, Ge and Sn, for x and y ranging from 0–12 at. % and 0–20 at. %, respectively. The important finding is that all $GeSn_y$ layers with $y < 10$, including pure Ge ($y = 0$), grown directly on a cubic $Ge_{0.9}Sn_{0.1}$ or on a partially relaxed $Ge_{1-x}Sn_x$ ($y < x \geq 10$) undergoes the desired indirect to direct transition: the conduction band minimum shifts from the L valley to the Γ valley forming a direct bandgap at the center of the Brillouin zone. This strain-induced transition will significantly enhance the tunneling probability. Moreover, the simulation results allow the selection of Si and Sn concentrations which optimize the band alignments with reasonable band-offsets between strained Ge Γ-valley and the $Si_xGe_{1-x-y}Sn_y$ L-valley. An example of a Tunnel-FET structure is shown in Fig. 1 where the following bandgaps were calculated for: $E_{\Gamma GeSn} = 0.452$ eV for relaxed $Ge_{0.9}Sn_{0.1}$, $E_{\Gamma Ge} = 0.547$ eV for the tensely strained Ge and $E_{\Gamma SiGeSn} = 0.684$ eV for tensile strained $Si_{0.12}Ge_{0.84}Sn_{0.04}$. The channel to drain bandgap offset can be even increased by employing $Si_{0.20}Ge_{0.76}Sn_{0.04}$ which possess $E_{\Gamma SiGeSn} = 0.812$ eV. These are within the spread of available experimental or theoretical data from the literature. For example, the linear expression with tolerance limits, found from fitting to experiments for relaxed ternary SiGeSn alloys,[9] predicts a gap of 1.03 eV for $Si_{0.12}Ge_{0.84}Sn_{0.04}$. The unstrained binary GeSn is predicted to show the indirect-direct crossover between 7% (Ref. 10) and a bit over 10% (Ref. 11) Sn (with a gap of ∼0.450eV (Ref. 11)),

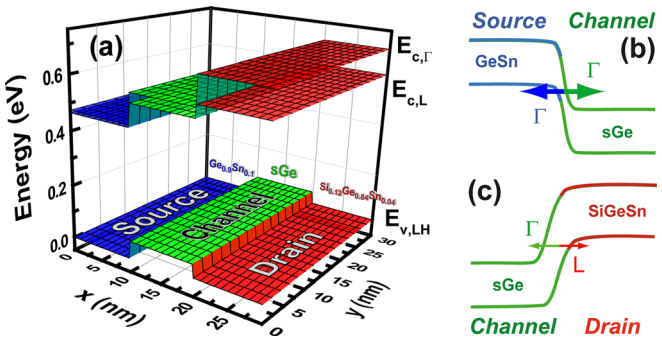

FIG. 1. (a) Calculated band diagram of a relaxed $Ge_{0.9}Sn_{0.1}$/tensely strained Ge/relaxed $Si_{0.12}Ge_{0.84}Sn_{0.04}$ heterostructure and schematic illustration of the main band-to-band tunneling processes, (b) $\Gamma \rightarrow \Gamma$ at the source side, and (c) $L \rightarrow \Gamma$ at the drain side.

compared to 10% Sn and 0.465 eV from the expressions we have used.

This concept fulfills the requirement of a small effective tunneling barrier within the direct bandgap materials (Fig. 1(b)), in order to achieve high on-state current and reduces both, the ambipolar behavior and the leakage due to the indirect and larger bandgap of the SiGeSn drain (Fig. 1(c)). We expect unipolar characteristics since the tunneling probability decreases rapidly with increasing barrier height, which can reach 1 eV for relaxed, Si rich SiGeSn.[8,9] Moreover, the heterostructure concept is regarded as the most scalable approach for solving the ambipolar problem.[12]

In the following, we demonstrate the single crystal growth of such sophisticated epitaxial stacks as suggested by the band engineering simulations. The tunnel region formed by relaxed GeSn with Sn content up to 12 at. % and strained Ge layers with thicknesses up to 50 nm and strain level of 1.2% is first presented. The pseudomorphic growth of SiGeSn with optimized Si to Sn concentration ratios on Ge is then addressed.

The (Si)Ge(Sn) layers were grown using an industry compatible metal cold-wall Reduced Pressure AIXTRON TRICENT® reactor (RP-CVD) with a showerhead for 200/300 mm wafers.[13] The epitaxial layers were grown using Si_2H_6, Ge_2H_6 (10% diluted in H_2) and $SnCl_4$ precursors, and N_2 carrier gas, which warrant reasonable growth rates at growth temperatures as low as 375 °C.[13,14] In this configuration, GeSn layers with up to 10 at. % Sn concentration on Si(100) substrates were obtained.[13] The use of these layers as tunneling source in Tunnel-FETs sets high requirements for single crystalline quality and pseudomorphic growth of strained Ge layers. The smaller lattice mismatch between GeSn and Ge compared to Si, substantially reduces the defect density observed for GeSn layers grown directly on Si substrates. In this respect we have used low defect density Ge virtual substrates (VSs) on Si(001) substrates.[15,16]

The crystalline quality and composition of the (Si)Ge(Sn) layers were investigated by Rutherford Backscattering Spectrometry in the ion channeling mode (RBS/C) and the strain relaxation of GeSn layers by X-Ray Diffraction Reciprocal Space Mapping (RSM) around the asymmetric (224) reflection. The insets of Fig. 2 show the diffractograms obtained for 30 nm, 90 nm, and 195 nm thick $Ge_{0.92}Sn_{0.08}$ layers. Based on the lattice constants extracted for the GeSn crystals, we calculated a degree of strain relaxation of 0% (fully strained), 50%, and 78%, respectively. Cross-section transmission electron (XTEM) micrographs (Fig. 2) provide evidence for pseudomorphic growth of the 30 nm layer and misfit dislocation formation at the GeSn/Ge VS interface, typical for the strain relaxed layers.

The relaxed GeSn layers were used as buffers for the epitaxial growth of tensile strained Ge layers and RSM was employed to assign the elastic strain in the Ge layers by measuring the in-plane and out-of-plane lattice constants (see Fig. 3). A biaxial tensile strain of about 0.7% was found for a Ge layer grown on a $Ge_{0.92}Sn_{0.08}$ buffer and 1.2% on a $Ge_{0.904}Sn_{0.096}$ buffer. The strain corresponds to the theoretical value expected for lattice matched Ge growth on a crystal lattice of 78% relaxed $Ge_{0.92}Sn_{0.08}$ and 77% relaxed $Ge_{0.904}Sn_{0.096}$ buffers, respectively. Figure 3(a) presents the RSM image of 50 nm strained Ge layer on 255 nm $Ge_{0.904}Sn_{0.096}$ buffer grown at 375 °C. The determined in-plane and out-of-plane lattice constants indicate pseudomorphic Ge growth on top of the GeSn buffer, as evidenced by the XTEM micrograph in Fig. 3(a) as well. Furthermore, Raman spectroscopy measurements were carried out to investigate the grown layers. Based on the measured shifts, $\Delta\omega$, towards lower wavenumbers in the Raman spectra, Fig. 3(b), the strain values were calculated as:[17] $\Delta\omega = b\epsilon_{\parallel}$, with $\epsilon_{\parallel}$ as biaxial strain and $b = -415\,cm^{-1}$.[18] The calculated strain values confirm the results obtained by RSM. The perfect symmetry of the Ge vibration modes and the low full width at half maximum values (see inset), similar to those in high quality high Ge content SiGe layers, are an evidence of single crystalline quality.

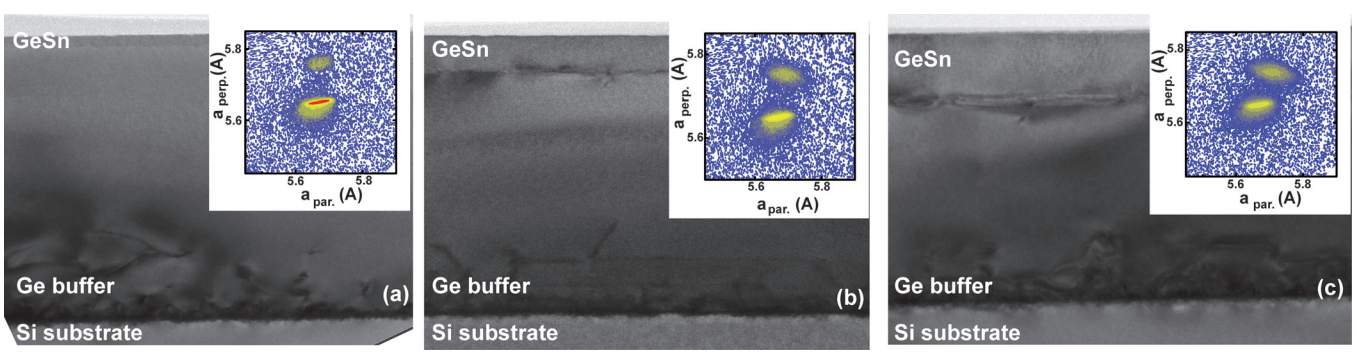

FIG. 2. XTEM micrographs of (a) 30, (b) 90 and (c) 195 nm thick $Ge_{0.92}Sn_{0.08}$ layers which show 0% (fully strained), 50% and 78% strain relaxation. The corresponding RSM diffractograms used for the elastic strain determination are shown as insets.

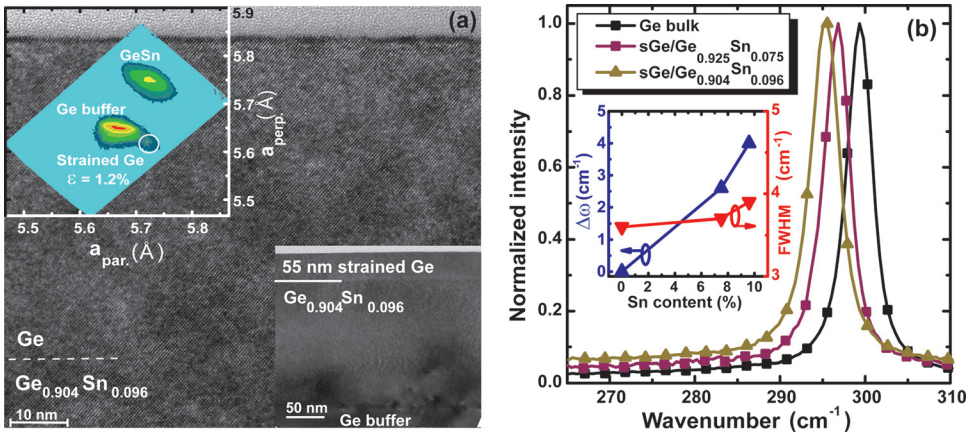

FIG. 3. (a) The TEM micrograph of 55 nm strained Ge layer grown on 255 nm $Ge_{0.904}Sn_{0.096}$ buffer on Ge VS. The reciprocal space mapping around the (004) reflection is shown in the inset. A tensile strain of about 1.2% is deduced for the top Ge layer. (b) Raman spectra of the Ge layers on $Ge_{0.925}Sn_{0.075}$ and $Ge_{0.904}Sn_{0.096}$ buffers, taken at a wavelength of 488 nm. The Raman shift and the FWHM versus Sn content are presented in the inset.

Incomplete strain relaxation, however, raises the question if a direct-gap can be reached, and these layers can be used as proposed. However, more important here is $\Delta E_{\Gamma L} = E_{\Gamma} - E_{L}$, which defines the "directness" of a semiconductor at room temperature. Figure 4 shows the epitaxial growth of a $Ge_{0.88}Sn_{0.12}$ layer and its directness for different degree of strain relaxation. The fully relaxed $Ge_{0.88}Sn_{0.12}$ has a direct-gap of 402 meV, and an indirect of 433 meV. A strain relaxation of 75% implies that the layer is under biaxial compressive strain of −0.6% corresponding to a fully relaxed GeSn layer with 9 at. % Sn. The compressive strain renders the layer indirect but the Γ valley is at 477 meV, and the L valley at 469 meV. The difference $\Delta E_{\Gamma L}$ amounts then to only 8 meV, much is well below k_BT enabling a "pseudo direct-gap" at room temperature. The results of Fig. 4 suggest that $Ge_{1-x}Sn_x$ layers with $x_{Sn} > 9$at. % allow for certain compressive strain to profit from the directness as discussed above.

The final ingredient of the proposed Tunnel FET heterostructure is the SiGeSn drain. As mentioned in the introduction, large bandgaps are required to minimize the ambipolarity of tunnel devices. Theoretical considerations of Moontragoon *et al.*[8] and Beeler *et al.*[9] indicated that cubic

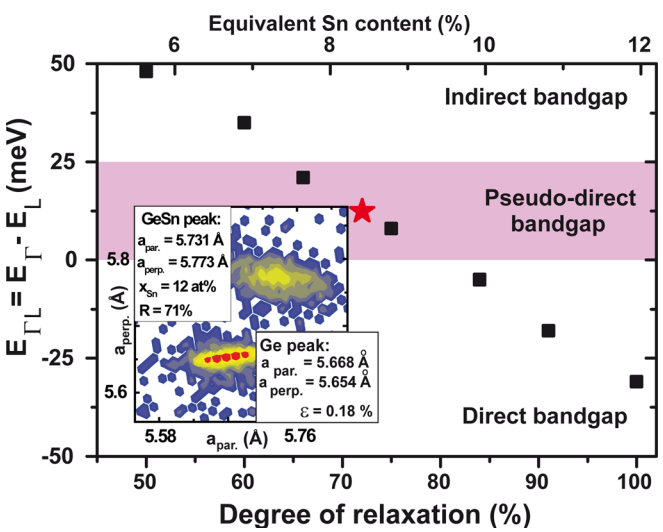

FIG. 4. Calculated "directness" $\Delta E_{\Gamma L}$ for a $Ge_{0.88}Sn_{0.12}$ layer versus the degree of relaxation (lower scale) or corresponding Sn content of a fully relaxed GeSn layer (upper scale). The RSM diffractogram of a 300 nm $Ge_{0.88}Sn_{0.12}$ layers is presented as inset. The relaxation degree corresponds to 71%.

SiGeSn alloys with Si contents in the range of 10–20 at. % and Sn concentration below 5 at. %, possess an indirect bandgap above 0.95 eV, much larger than 0.5 eV as our simulations indicate for the strained Ge channel grown on effective $Ge_{0.91}Sn_{0.09}$ lattice, where Ge has a direct-gap. Here, we show an example of the single crystal growth of a $Si_{0.12}Ge_{0.84}Sn_{0.04}$ layer on a thin Ge buffer (Fig. 5(a)).[13] Only a single diffraction peak besides the Si one is observed, indicating an identical crystal lattice, in-plane and out-of-plane, for $Si_{0.12}Ge_{0.84}Sn_{0.04}$ and Ge VS. RBS channeling (not shown here) indicates a single crystalline $Si_{0.12}Ge_{0.84}Sn_{0.04}$ layer with excellent minimum yield values for both Si and Sn. Previous studies of SiGeSn ternaries reported a perfect lattice match to Ge for Si/Sn ratio of 3.65:1.[19] Note that the thin Ge buffer exhibits a slightly compressive strain, and hence a tetragonal, rather than cubic lattice.

In the proposed structure, the SiGeSn layer is under high tensile strain which, however, does not change the band alignment type but the bands off-sets. The bandgap of SiGeSn increases with the increase of the Si content and decreases with the increasing tensile strain. Table I summarizes the band positions for different GeSn/Ge/SiGeSn combinations considering pseudomorphic growth. On a GeSn lattice corresponding to 10% Sn, obtained by 100% relaxation of $Ge_{0.9}Sn_{0.1}$ or 85% relaxation of $Ge_{0.88}Sn_{0.12}$, the strained Ge (here channel) adapts a direct gap. Regarding the drain side, fully strained $Si_{0.12}Ge_{0.84}Sn_{0.04}$ has a bandgap of 575 meV and a bandgap difference to strained Ge of about 92 meV. These values increase to 620 meV and about 137 meV, respectively, for a high Si content of 20 at. % in the SiGeSn layer. Taking also into account that for SiGeSn is always indirect (for the indicated Si and Sn ranges), a very low BTBT current is expected at drain side. As a proof of concept, a complete GeSn/strained Ge/SiGeSn structure is presented in Fig. 5(b) showing the RBS spectrum measured at He^+ ion energy of 3 MeV to allow the separation of the Sn signals from the other contributions. The good interface quality is demonstrated by the sharp Si, Ge, and Sn signals in the SIMS spectrum (inset Fig. 5(b)).

In summary, a vertical heterostructure based on two direct bandgap semiconductors, GeSn and strained Ge for source and channel, and SiGeSn as a large bandgap indirect semiconductor for drain has been proposed. We have presented the growth of lattice matched relaxed $Ge_{0.9}Sn_{0.1}$/strained Ge as well as Ge/$Si_{0.12}Ge_{0.84}Sn_{0.04}$ structures with

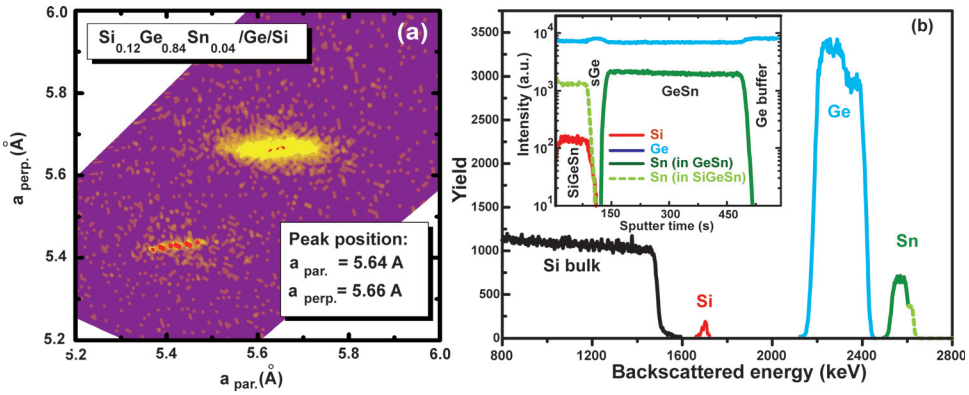

FIG. 5. (a) RSM of a 52 nm $Si_{0.12}Ge_{0.84}Sn_{0.04}$/Ge VS sample, showing the overlap of Ge and $Si_{0.12}Ge_{0.84}Sn_{0.04}$ layers diffraction patterns and the single crystalline quality of the layers, respectively. (b) RBS spectrum with SIMS spectrum (inset) of a complete GeSn/strained Ge/SiGeSn Tunnel-FET heterostructure.

TABLE I. Lattice constant, bandgap, Γ and L valleys energy, light hole (LH) and heavy hole (HH) energies, the bandgap difference and the "directness" for different Tunnel-FET possible structures. The lattice (Sn%) represents the equivalent fully relaxed lattice in Sn at. % of a corresponding to the partial relaxed GeSn layer.

Layer	Lattice (Sn%)	Eg (meV)	E_{Γ} (meV)	E_{L} (meV)	E_{HH} (meV)	E_{LH} (meV)	ΔE_G (meV)	$\Delta E_{\Gamma L}$ (meV)
$GeSn_{0.12}$	10%	425	452	457	27	−2	18	−5
$GeSn_{0.10}$	10%	465	465	474	0	0		−9
Ge	10%	483	547	582	−137	64	137	−35
$Si_{0.2}GeSn_{0.04}$	10%	620	812	636	−213	16		176
$Si_{0.12}GeSn_{0.04}$	10%	575	684	591	−161	16	92	93

excellent crystalline quality, similar to state-of-the-art SiGe layers. However, even if a direct bandgap in GeSn and strained Ge is not reached, strongly enhanced tunneling is expected since tensile strain enables (i) strong directness of the pseudo direct-gap layers, (ii) a significantly increased electron population of the Γ valley, meaning increased direct tunneling component, and (iii) a smaller effective mass, since the band curvature of the valley is larger than that of the L valley.[20] These features make the strained Ge an excellent choice for Tunnel-FETs, not only, as mostly envisaged, for optoelectronic applications. Moreover, the ability to grow and combine $Ge_{1-x}Sn_x$ ($x < 12\%$) and $Si_yGe_{1-x-y}Sn_x$ layers may allow the development of advanced epitaxial structures for new applications, like laser structures.[21]

[1]A. M. Ionescu and H. Riel, Nature **479**, 329 (2011).
[2]J. Knoch and J. Appenzeller, in *Device Research Conference Digest* (IEEE, 2005), p. 153.
[3]K. Kao, A. Verhulst, W. Vandenberghe, B. Sorée, G. Groeseneken, and K. De Meyer, IEEE Trans. Electron Devices **59**, 292 (2012).
[4]K. L. Low, Y. Yang, G. Han, W. Fan, and Y. Yeo, J. Appl. Phys. **112**, 103715 (2012).
[5]W. G. Vandenberghe, B. Sorée, W. Magnus, G. Groeseneken, and M. V. Fischetti, Appl. Phys. Lett. **98**, 143503 (2011).
[6]D. Mohata, B. Rajamohanan, T. Mayer, M. Hudait, J. Fastenau, D. Lubyshev, A. W. K. Liu, and S. Datta, IEEE Electron Device Lett. **33**, 1568 (2012).
[7]P. Moontragoon, P. Pengpit, T. Burinprakhon, S. Maensiri, N. Vukmirovic, Z. Ikonic, and P. Harrison, J. Non-Cryst. Solids **358**, 2096 (2012).
[8]P. Moontragoon, R. A. Soref, and Z. Ikonic, J. Appl. Phys. **112**, 073106 (2012).
[9]R. T. Beeler, C. Xu, D. J. Smith, G. Grzybowski, J. Menéndez, and J. Kouvetakis, Appl. Phys. Lett. **101**, 221111 (2012).
[10]R. Chen, H. Lin, Y. Huo, C. Hitzman, T. I. Kamins, and J. S. Harris, Appl. Phys. Lett. **99**, 181125 (2011).
[11]H. P. L. de Guevara, A. G. Rodríguez, H. Navarro-Contreras, and M. A. Vidal, Appl. Phys. Lett. **84**, 4532 (2004).
[12]T. Krishnamohan, D. Kim, S. Raghunathan, and K. Saraswat, Tech. Dig.—Int. Electron Device Meet. **67**, 7 (2008).
[13]S. Wirths, D. Buca, G. Mussler, A. T. Tiedemann, B. Holländer, P. Bernardy, T. Stoica, D. Grützmacher, and S. Mantl, ECS J. Solid State Sci. Technol. **2**(5), N99–N102 (2013).
[14]S. Wirths, D. Buca, A. T. Tiedemann, P. Bernardy, B. Holländer, T. Stoica, G. Mussler, U. Breuer, and S. Mantl, Solid-State Electron. **83**, 2 (2013).
[15]V. A. Shah, A. Dobbie, M. Myronov, and D. R. Leadley, Solid-State Electron. **62**, 189 (2011).
[16]J. M. Hartmann, A. Abbadie, N. Cherkashin, H. Grampeix, and L. Clavelier, Semicond. Sci. Technol. **24**, 055002 (2009).
[17]Y. Bai, K. E. Lee, C. Cheng, M. L. Lee, and E. A. Fitzgerald, J. Appl. Phys. **104**, 084518 (2008).
[18]Y.-Y. Fang, J. Tolle, R. Roucka, A. V. G. Chizmeshya, J. Kouvetakis, V. R. D'Costa, and J. Menéndez, Appl. Phys. Lett. **90**, 061915 (2007).
[19]V. D'Costa, Y.-Y. Fang, J. Tolle, J. Kouvetakis, and J. Menéndez, Phys. Rev. Lett. **102**, 107403 (2009).
[20]M. V. Fischetti and S. E. Laux, J. Appl. Phys. **80**, 2234 (1996).
[21]G. Sun, R. A. Soref, and H. H. Cheng, J. Appl. Phys. **108**, 033107 (2010).